Chapter 8

The Effect of Clay Type on the Physicochemical Properties of New Hydrogel Clay Nanocomposites

Tatiana Munteanu, Claudia Mihaela Ninciuleanu, Ioana Catalina Gifu, Bogdan Trica, Elvira Alexandrescu, Augusta Raluca Gabor, Silviu Preda, Cristian Petcu, Cristina Lavinia Nistor, Sabina Georgiana Nitu and Raluca Ianchis

Additional information is available at the end of the chapter

http://dx.doi.org/10.5772/intechopen.74478

Abstract

This study focuses on the investigation of clay type effect on the final properties of semi-interpenetrated Salecan/poly(methacrylic acid)/clay hydrogel nanocomposites. Previous studies have indicated that the presence of clay in polymer composites leads to better swelling capacity and mechanical properties as functions of clay type. On the other hand, Salecan, which is a water soluble extracellular polysaccharide, was proved to assure greater flexibility to hydrogels. These properties recommend clay and Salecan for semi-interpenetrated hydrogels preparation with specific application in biomedicine. The purpose was to determine the most suitable type of clay as well as Salecan influence for developing the desired water retention/delivery ability and mechanically enhanced semi-interpenetrating polymer network (SIPN) nanocomposites. For our investigations, we have chosen commercially available montmorillonite (ClNa) and different commercial organomodified clay (Cl30B, Cl20A and Cl15A). Several analyses results (FTIR, TGA, DMA, XRD, microscopy and swelling studies) demonstrated that not only the presence of Salecan but also the clay type influenced the structure and properties of the final nanocomposites.

Keywords: clay mineral, Salecan, poly(methacrylic acid), hydrogel, nanocomposites

1. Introduction

Hydrogels can be defined as three-dimensional cross-linked polymer networks that have the property of swallowing a substantial amount of water without dissolving as an effect of their physical and/or chemical cross-linking matrix architecture [1, 2]. Besides excellent swelling capacity, other features of hydrogels include an outstanding biocompatibility, high permeability for water-soluble agents and adjustable mechanical properties. Consequently, these materials have been studied extensively for medical application purposes such as tissue engineering, drug delivery systems and biosensor fields [3]. Lately, polysaccharide-constructed hydrogels have gained more attention. The main disadvantage of polysaccharide hydrogels is the lack of mechanical strength, and for this reason, the introduction of a rigid synthetic polymer in order to develop interpenetrating or semi-interpenetrating polymer network hydrogels (IPN/SIPN) with improved strength is being recently studied. IPN or SIPN differs from other multicomponent systems through the highly intimate contact between the polymers, though no chemical bond exists between them. The unique properties of the final nanomaterials are given by the entanglement between the polymer chains. Moreover, the porous morphology of the structure allows numerous applications in various fields. The challenge of synthesizing clay mineral-containing nanocomposite hydrogels in an effective way is still present. More attention is necessary to be paid for combining the strong aspects of layered clay minerals and those of the polymers where both can be modified and functionalized as function of the final materials desired to be manufactured.

Salecan is a polysaccharide that possesses a high number of hydroxyl groups on the main chain, allowing this way to be accordingly managed in SIPN architecture. Antioxidant and nontoxic character as well as biocompatibility and biodegradability make it highly suitable for drug delivery purposes. Poly(methacrylic acid) (PMAA) is a synthetic polymer often investigated for being a desirable component of a SIPN. Methacrylic acid (MAA) is a water-soluble monomer that has the ability of polymerizing via *free radical polymerization* under convenient condition. PMAA is a synthetic polyelectrolyte capable of donating or accepting protons upon pH changes, accompanying reversible conformational alterations between the collapse and extension state [3]. Nontoxicity and outstanding mechanical strength sustain its usage in pharmaceutical industry.

Regarding Salecan/PMMA semi-IPN, the study conducted by Qi et al. [3] showed, besides a successful incorporation of the components in a semi-IPN architecture, several features: (1) Salecan addition leads to a better thermal stability of the network; (2) an increment in the Salecan dose resulted in an increase in the average pore size, resulting in an enhanced hydrophilicity of the construction; at the same time, an increase in the cross-linker agent leads to a decrease in pore size as a consequence of a higher density of the network; (3) Salecan facilitates the penetration of water molecules into the network, thus higher equilibrium swelling ratio is obtained while the cross-linker has a completely opposite effect; (4) the pH effect of swelling is assigned to the protonation and ionization balance of the carboxyl acid groups appearing in the hydrogel chains, whose pKa value was approximately 5.5; and (5) at lower pH, the acid groups in the hydrogel cannot be easily ionized.

http://dx.doi.org/10.5772/intechopen.74478

The hydrogen bonds between the hydroxyl groups in Salecan and the protonated acid groups in PMAA restrained the swelling of the hydrogel. When the pH is increased, the carboxyl groups of PMAA chains dissociated, undermining the H-bonds between the Salecan and PMAA chains.

On the other hand, clay nanocomposites have also attracted attention worldwide. The contact between the polymer and clay leads to better thermal and mechanical stability, durability or reduced permeability to small molecules and solvent uptake [4], thus being effectively used to modify drug delivery systems. As a hydrogel network component, clays have proven to act as a trap for the drug that would be released, preventing uncontrolled diffusion of the drug from the gel network and offering a better control of the release. In absence of clay, the drug-loaded hydrogels suffer a burst type of delivery [5]. Over the years, numerous studies demonstrated the outstanding properties of the clay-polymeric materials [6–8]. For instance, Pinnavaia et al. reported increased tensile strength, modulus and heat distortion temperature of polymer-clay nanocomposites compared to the simple polymer [6]. Park et al. showed great enhancement in the release rate of the drug for the inorganic–organic hybrid successfully realized by intercalating donepezil molecules into smectite clays [9]. The improvement achieved with the clay inclusion is better defined when the silicate lamellas tend to an intercalated to exfoliated structure.

All the aforementioned features and described techniques lead to the conclusion that on one hand, we have the semi-IPNs, in particular, Salecan/PMMA with outstanding potential for being designed as drug delivery systems, and on the other hand, there are clay-polymeric nanocomposites intended for various medical applications. Therefore, we considered the advantages of both systems and decided to develop a novel synergic system suitable for oral delivery of drugs, by combining the hydrophilic networks composed of poly(methacrylic acid) and Salecan with clay mineral nanoparticles. The designed polymer nanocomposite carriers would be able to provide cancer treatment by direct delivery of the medicine to the colon. More than that, we aimed to investigate the effect of the initial clay composition upon the final properties of Salecan/PMMA semi-IPN. In most of the cases, the developing of clay/polymer nanocomposites with sodium montmorillonite (ClNa) was envisaged.

Interesting investigations, in our opinion, would be regarding the structures obtained with ClNa but with hydrophobic montmorillonites as well. As the clays are basically hydrophilic compounds, the only way to turn them into a structure compatible with hydrophobic network is to functionalize them using ammonium salts [10] or by sol–gel process with various long alkyl chain silanes [11, 12]. The synthesis of various *in house* advanced modified Cloisites were previously reported starting from commercial clay by edge covalent bonding at the clay edges [13]. By measuring the static contact angle values for water, the modified clay minerals proved to have an enhanced hydrophobic behavior [12, 14]. But for this study, we have chosen the commercially available Cloisite Na and organomodified montmorillonite with different ammonium salts: (methyl, tallow, bis-2-hidroxyethyl)-Cloisite 30B, (dimethyl, dehydrogenated tallow)-Cloisite 20A and (dimethyl, dehydrogenated tallow)-Cloisite 15A.

These hydrophilic-hydrophobic complex systems are foreseen to find application in controlled drug release where *co*-delivery of polar-unpolar substances at the target site is mandatory.

2. Experimental

2.1. Materials

Commercial clays ClNa, Cl30B, Cl20A and Cl15A were kindly offered by Southern Clay Products Inc. PMAA (polymethacrylic acid, Janssen Chimica), Salecan (Souzhou Chemicals), N, N′-methylenebisacrylamide (Sigma Aldrich) and ammonium persulfate (Sigma Aldrich) were used as received.

2.2. Synthesis of PMAA/Salecan/clay nanocomposites

In order to obtain the proposed systems, two main types of hydrogels were manufactured: PMAA/clay hydrogel nanocomposites and PMAA/Salecan/clay hydrogels. The method used was adapted from the one found in the literature [3], as follows: primarily, a 0.2 g clay (ClNa, Cl30B, Cl20A and 15A) was dispersed in 14 ml of deionized water under magnetical stirring (around 800 rpm) and room temperature for 15 min. Thus, the clay dispersion was obtained and ultrasonicated for 5 min. When the hydrogels with Salecan were prepared, 0.16 g of Salecan powder was added, and the system was kept under mechanical stirring for another 15 min followed by 1 min ultrasonication.

For the PMAA/clay nanocomposites, this step was omitted. As the mass became homogenous and cooled, 2 ml MAA and 2 ml BIS (1%, w/v) were added under continuous stirring for 10 min followed by 10 min ultrasonication in an ice bath. Two milliliter APS (1.2%, w/v) was added, keeping the mass under magnetical stirring for another 5 min. The system was injected for polymerization into our own-designed glass mold. The mold was introduced into a thermostated water bath at 70°C (the desired temperature for the polymerization to occur) for 6 h.

The obtained hydrogels were cut into pieces and immersed into deionized water for 7 days. The water was changed two times a day in order to assure that the residual monomers were removed. As for analyses, the fabricated hydrogel nanocomposites were cut with an eyelet punch. One part of the cuts was deposed on polyethylene foils for water evaporation at ambient temperature for several days and the other part was freeze dried.

3. Characterization

3.1. Fourier transform infrared spectroscopy

The FTIR spectra were obtained by a Fourier transform infrared spectrophotometer BRUKER Tensor on ATR mode in the range of the scanning wave numbers 4000–400 cm^{-1} with a 40 scans per sample cycle and a resolution of 4 cm^{-1}. Milled samples were used for FTIR analyses.

http://dx.doi.org/10.5772/intechopen.74478

3.2. X-ray diffraction

Powder X-ray diffraction was used for phase identification of the crystalline material and to determine the lattice parameters of the crystal structure. A multifunctional system powder X-ray diffractometer, Rigaku Ultima IV (Tokyo, Japan), was used to perform the measurements. The equipment conditions were as follows: X-ray generator was operated at 40 kV voltage and 30 mA current, using Cu target (CuKα radiation, λ = 1.5406 Å); the goniometer was set in parallel beam geometry system, with cross beam optics (CBO), θ-θ scanning mode and with a step width of 0.02°; a scintillation counter was used. For low angle measurements, the optics used were DS and SS (divergence and scattering slits) = 1°, RS (receiving slit) = 0.2° and receiving side Soller slit 0.5°, collecting data between $0.6 < 2\theta < 6°$ measuring range, with a scanning speed of 1°/min. For wide angle measurements, the optics used were DS (divergence slit) = 1°, SS and RS (scattering and receiving slits) = open and receiving side Soller slit 0.5°, collecting data between $3 < 2\theta < 50°$ measuring range, with a scanning speed of 2°/min. The measurements were performed in the continuous mode, at room temperature and atmospheric pressure.

3.3. Thermal gravimetric analysis

Thermogravimetric (TGA) measurements were performed with a TGA Q5000 instrument. The samples were heated, in nitrogen atmosphere 10 ml/min with a rate of 10°C/min.

The isotherms of equilibrium swollen hydrogel disks were carried at 37°C for 10 mL/min in nitrogen atmosphere. All experiments were realized in triplicate.

3.4. Swelling behavior measurements

Swelling studies of semi-IPNs were conducted by immersing the dried samples in deionized water at 37± 1°C. The samples were removed from the thermostatic bath at regular intervals of time, their surface was dried with filter paper and then weighed; afterward, they were immersed into the same recipient.

The swelling degree (*SD*) was calculated using Eq. (1):

$$SD = (Wh - Wi)/Wi \quad (1)$$

where *Wh* is the weight of swelled hydrogel at a certain time and *Wi* is the weight of initial dried hydrogel. All experiments were performed in triplicate.

3.5. Electron microscopy analyses: SEM and TEM

ESEM-FEI Quanta 200 (Eindhoven, Netherlands) instrument was used to record SEM images in low vacuum mode with GSED detector. Micrographs were taken in vacuum conditions, operating pressure of 2 torr, 25–30 KV accelerating voltage.

The morphologies of PMAA nanocomposites were obtained by transmission electron microscopy using TEM, Tecnai™ G2 F20 TWIN Cryo-TEM, FEI Company™, at 200 kV acceleration voltages. Powdered samples were deposited on carbon film grids.

3.6. Mechanical properties

Dynamic mechanical analysis (DMA) was performed using the DMA-Q 800 device (TA Instruments New Castle, DE, USA). Freeze-dried hydrogels were analyzed in "Temperature Ramp" mode and swollen hydrogels in DMA Multi-Frequency-Strain "Frequency sweep-isothermal." Dual cantilever-powder clamp was used for freeze-dried hydrogels and compression clamp was used for hydrogels. Hydrogels disk were cut with an eyelet (part of DMA-Q 800 Dynamic Analyzer compression set) before analyses, the dimensions of the analyzed specimens being about 12.5 mm diameter. Rectangles of 60 mm × 12.77 × 2–3 mm were used for lyophilized hydrogels. These were then measured with a caliper in order to enter the initial values. "Isothermal" mode was carried out at 30°C with 4 μm oscillation amplitude for 120 min from 0.1 to 10 Hz at 11 frequencies (frequency sweep segment repeat for 10 times). A 14.5 mm compression plate was used for all samples. A 0.01 N compressive static force was applied to the specimen to ensure that the upper compression plate did not lose contact with the sample. The measurements were repeated for three times.

For the "Temperature ramp" mode, the temperature ranged from 275 to 300°C/min, oscillation amplitude of 20 μm, 1 Hz frequency and 0.5 sampling.

DMA-Q 800 used Universal Analysis 2000 for calculating dynamic mechanical properties and exports the data for plotting the investigated properties as a function of time, temperature and frequencies.

4. Results and discussion

4.1. Fourier transform infrared spectroscopy

The presence of montmorillonite in the polymer matrix was checked by FTIR analysis (see **Figure 1**, only PMAA-ClNa and Cl15A data are presented here). FTIR spectra of Cloisites show the presence of clay characteristic peaks, confirmed also by the literature data [12, 15]. For all four types of montmorillonites, around 3633 cm^{-1} we noticed the OH stretching of latex water. The peak from 1011 cm^{-1} with a shoulder at 921 cm^{-1} was attributed to Si–O stretching vibration while the Si–O bending vibration was identified in the 400–600 cm^{-1} area, more exactly 518 cm^{-1} and 454 cm^{-1}. The difference between the ClNa and the modified clays (Cl30B, Cl15A and Cl20A) is given by the presence of additional peaks at 2926 cm^{-1} and 2852 cm^{-1}, specific for quaternary ammonium salts. As for the pure PMAA, its spectra reveal the characteristic peaks around 3000 cm^{-1} corresponding to the O–H stretching vibration and at 1737 cm^{-1} associated to CO group stretching vibration. At the wavelength of 2960–2875 cm^{-1}, the peaks for stretching vibration of methyl and methylene groups were found [16]. The absence of vinyl group stretching vibration at 1628–1692 cm^{-1} indicates that the polymerization occurred [15].

Referring to the spectra of Salecan, a broad peak was identified at 3329 cm^{-1}, being characteristic for O–H stretching vibration, as well as the intermolecular hydrogen bonding of the polysaccharide [17]. Peaks from the 800–1100 cm^{-1} area are assigned to polysaccharide structure and include C–OH stretching in the glucopyranose rings. More specifically, the band at

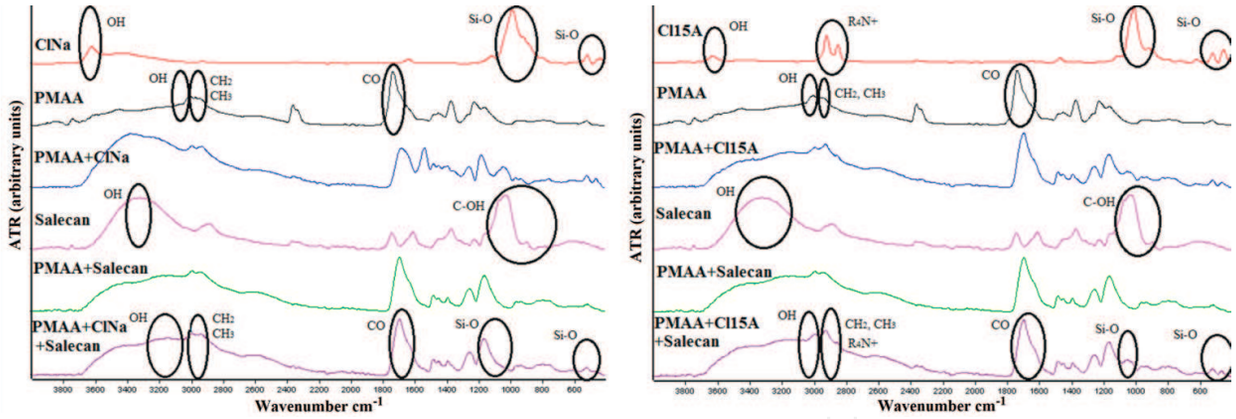

Figure 1. FT-IR spectra of the pristine clay/PMAA/PMAA-Cloisite/Salecan/PMAA-Salecan/PMAA-Salecan-Cloisite exemplified for ClNa and Cl15A.

1039 cm^{-1} was related to C–OH stretching in the glucopyranose ring, a broad, weak peak at 896 cm^{-1} suggested that D-glucopyranose had a β-configuration whereas the almost unidentifiable peak at 818 cm^{-1} confirmed the presence of small amounts of α-glucopyranose form.

Analyzing the spectra of the nanocomposites that have the modified montmorillonite as a component, alterations were noticed but also the preservation of some characteristic peaks. For instance, specific clay bands were observed. The Si–O–Si stretching vibration shifted from 1011 to 1050 cm^{-1} and the peaks from 400 to 600 cm^{-1} suffered a bathochromic shift. In the hydrogels, we found the Si–O bending and stretching vibration at 463 and 622 cm^{-1}, respectively.

For the composites prepared using modified montmorillonites, the bands at 2856 and 2925 cm^{-1} state that the quaternary ammonium salts are present in the network. At the same time, PMAA peaks were identified. Thus, we have C═O group stretching vibration, moved from 1737 to 1697 cm^{-1}(much lower intensity for 20A and 30B Cloisites), and the stretching vibration for methyl and methylene groups that slightly shifted to 2996–2925 cm^{-1} [18].

In a comparative analysis of PMAA and PMAA-Salecan bands, we noticed a change in the 2942 cm^{-1} peak. In the hydrogel structure, the peak broadens and suffers a decrease in sharpness, which can be explained by the formation of the intercalated structure between the polymer and the polysaccharide.

The fact that within the final structure, we find the skeleton of the compounds, we started with, serves as proof that the synthesis of semi-IPN hydrogels went successfully. The slight changes in wavelength and intensity could be explained by the interactions between the components of the hydrogels with the obtaining of a complex compact structure.

4.2. X-ray diffraction

XRD analysis was carried out in order to investigate the type of morphology of the clays, we study as well as the structure of final composites materials. According to the recorded data (**Figure 2**, I–IV), a broad peak centered at 2θ = 20° was observed in the XRD patterns of

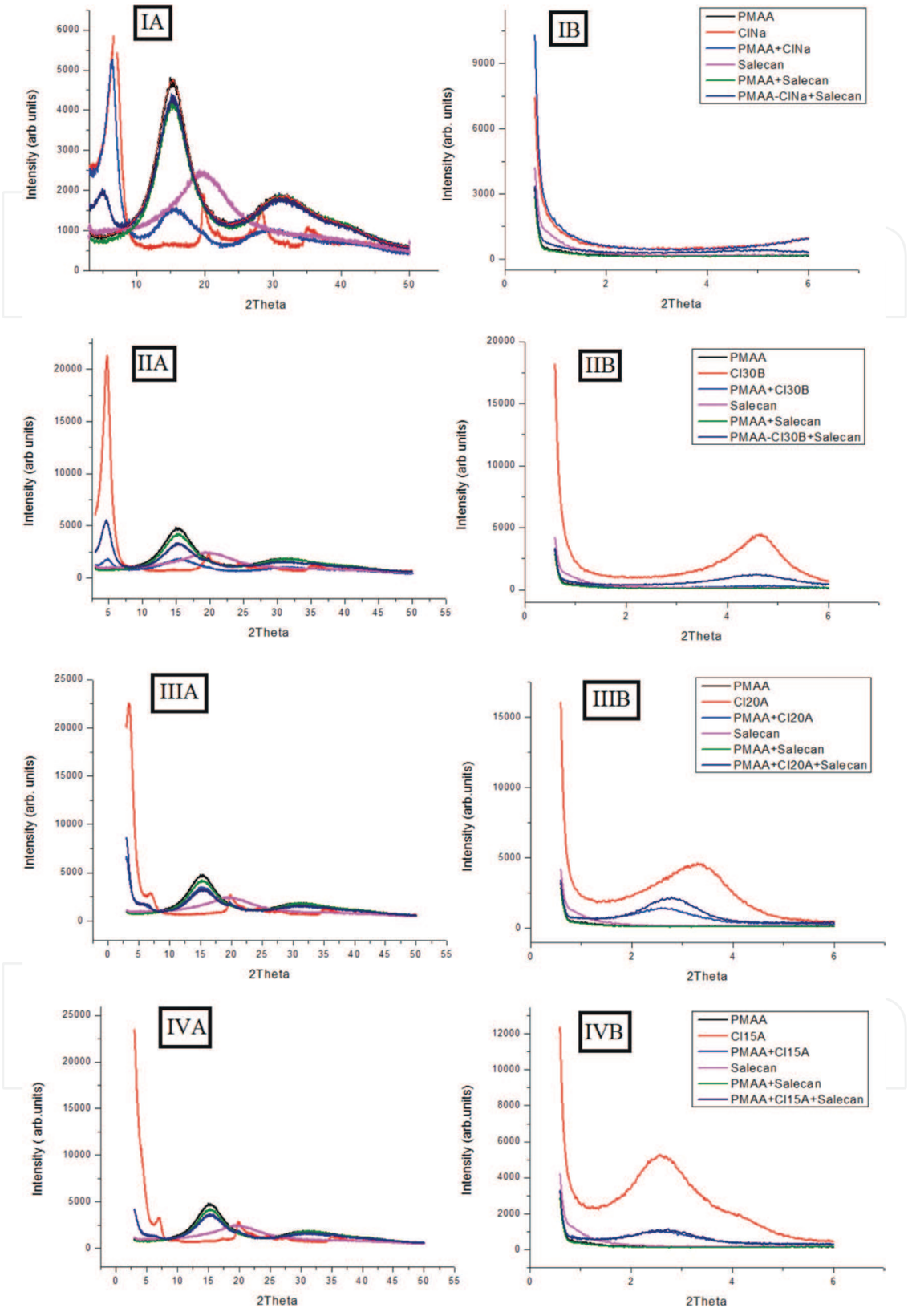

Figure 2. I. XRD results. I PMAA/ClNa/PMAA-ClNa/Salecan/PMAA-Salecan/PMAA-Salecan-ClNa; **II.** PMAA/Cl30B/ PMAA-Cl30B/Salecan/ PMAA-Salecan/ PMAA-Salecan-Cl30B; **III.** PMAA/Cl20A/PMAA-Cl20A/Salecan/PMAA-Salecan/ PMAA-Salecan-Cl20A; **IV.** PMAA/Cl15A/PMAA-Cl15A/Salecan/PMAA-Salecan/PMAA-Salecan-Cl15A; **A**: Wide angle; **B:** Low angle.

http://dx.doi.org/10.5772/intechopen.74478

Salecan. These results along with the literature data [3] prove that the Salecan had an amorphous structure. From the spectrum of pure PMAA hydrogel, it could be seen that the PMAA showed prominent diffraction peak posited around 2θ = 15°, suggesting the high crystallinity. The peak form and angle value are later noticed in the composites containing PMAA, with a slight loose in intensity due to the presence of Salecan and/or unmodified/modified clay.

XRD data of ClNa show the characteristic peak at 2θ = 7.3°. This peak is preserved in PMAA-ClNa spectra with a slight displacement at a lower angle (2θ = 6.7°). In the case of PMAA-ClNa-Salecan, the peak registered a decrease in intensity and was shifted to 2θ = 5°. The narrow, intense peak of ClNa present in PMAA-ClNa structure stands for a microcomposite, tactoid structure, while the decrease in intensity and broadening of the same peak in the PMAA-Salecan-ClNa hydrogels proves a highly intercalated network. The XRD pattern of Cloisite 30B reveals the main diffraction peak at 2θ = 4.9°. The same angle value of this peak is noticed in the PMAA-Cl30B composite as well as in the spectra of the final PMAA-Cl30B-Salecan hydrogel. A decrease in diffraction intensity and sharpness of the Cloisite peak in the composites leads to the conclusion that the montmorillonite tends to spread into an intercalated structure.

As for Cl20A and Cl15A, the characteristic diffraction peaks were identified at 2θ = 3.5° and 2θ = 2.3°, respectively. This was in conformity with the literature data [19] and stands for well-defined crystalline nature of Cloisites. The Cloisites have a tendency of spreading leading to slight intercalated layered structures of the PMAA-Cloisites and PMAA-Cloisites-Salecan, more obviously for the Cl15A.

The conclusion was deducted from the examination of Cloisite peaks that suffered an enlargement and decrease in intensity. From the all abovementioned Cloisites, Cloisite Na and Cloisite 30B seemed to have the highest degree of intercalation, whereas Cloisite 20A and Cloisite 15A formed only microcomposites (tactoid structure). What is interesting to notice is that in case of ClNa, the tactoid structure was perfectly preserved when PMAA-ClNa composites were synthesized but spread and turned into an intercalated-exfoliated structure once Salecan was added. As for other Cloisites, we do not have the same observation, for all of them, a little more intercalated morphology is noticed rather for PMAA-Cloisite composites than for final PMAA-Salecan-Cloisite hydrogel.

4.3. Thermal-gravimetric analysis

The thermal stability of the synthesized PMAA/Salecan hydrogel and hydrogel nanocomposites (PMAA/Salecan/clay) were examined by TGA analyses. Three steps of weight loss were registered (see **Figure 3**) with two maximum decomposition temperatures. The first weight loss is a result of water volatilization and the degradation of organic compounds [20].

The second and third steps are assigned to PMAA decomposition as well as the degradation of the main skeleton of Salecan. At this point, the polymer backbone is destroyed. Regarding the samples of nanocomposites obtained in the presence of simple/modified montmorillonite, some changes of the thermal stability of final materials were registered. These modifications were due to the presence of quaternary ammonium salts [4], more evident in the case of Cl15A and 20A. It is worth to mention that when Salecan was added, semi-interpenetrated networks were obtained, and the systems behave as homogenous architectures. Thus, the

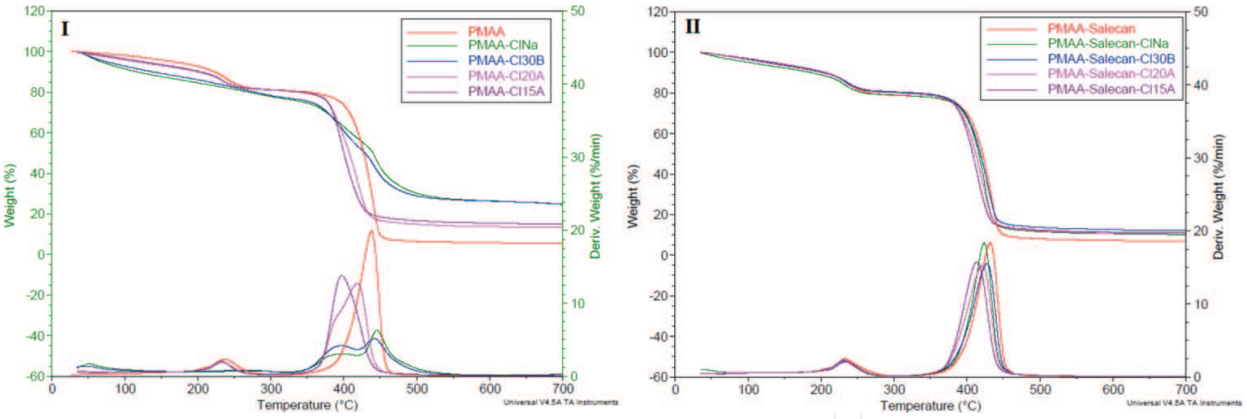

Figure 3. I. TGA results on samples without Salecan; **II.** TGA results on samples with Salecan.

energy consumed for nanocomposites thermal destruction is within the same range regardless of Cloisite type. The growing residue is related to the presence of inorganic filler and proves the inclusion of clay into hydrogels.

4.4. Swelling/deswelling behavior measurements

The data resulted from the swelling studies are shown in **Figure 4**. The swelling kinetics demonstrated that in all the cases, the capability to absorb water is much higher for nanocomposites than for PMAA/Salecan hydrogels. In the case of nanocomposite hydrogel based on ClNa, the swelling degree is about eight times higher than for pure hydrogel. Also, as can be noticed, the swelling degree (SD) decreases as we move from the hydrophilic ClNa to the most hydrophobic modified montmorillonite, Cl15A. Increasing the hydrophobicity of the clay, we designed a highly cross-linked hydrogel with intercalated/exfoliated silica lamellae, which lowers the freedom of polymeric chains and blocks the inflow of water to the network. This aspect should also be taken into consideration as the capability of hydrogels to absorb water is decisive for the drug loading and release as well as for the applications where superabsorbency is necessary.

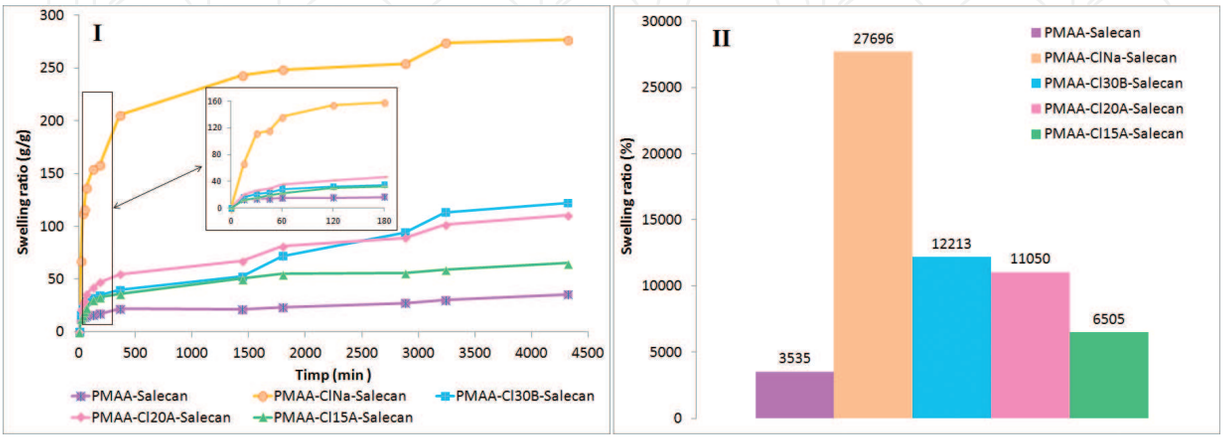

Figure 4. I. Time-dependent swelling profiles of the hydrogels; **II.** Representation of final degree ratio as a function of the clay type.

http://dx.doi.org/10.5772/intechopen.74478

TGA/DTG analyses provide information about deswelling behavior of the equilibrium swollen hydrogel samples. **Table 1** summarizes the characteristic values calculated from isotherm and derivative curves of the obtained samples. Derivative curves (see **Figure 5**) discover a slower weight change over time (50–80 min interval) in the following order: PMAA-Salecan, PMAA-Salecan-Cl20A, PMAA-Salecan-Cl15A and PMAA-Salecan-Cl30B/PMAA-Salecan-ClNa. The samples with clay exhibit higher dehydration rate and released

Sample	Isotherm curves, 37°C		Derivative curves	
	Time (min)	Weight (%)	$t_{1/2}$ (min)	t_{end} (min)
PMAA-Salecan	74.92	91.43	72.27	79.22
PMAA-Salecan-Cl Na	134.81	98.83	134.10	138.82
PMAA-Salecan-Cl 30B	103.14	96.20	101.96	106.68
PMAA-Salecan-Cl 20A	93.69	97.53	92.03	96.05
PMAA-Salecan-Cl 15A	99.83	95.47	97.70	104.09

Table 1. TGA/DTG data for PMAA-Salecan and PMAA-Salecan-clay nanocomposites, respectively.

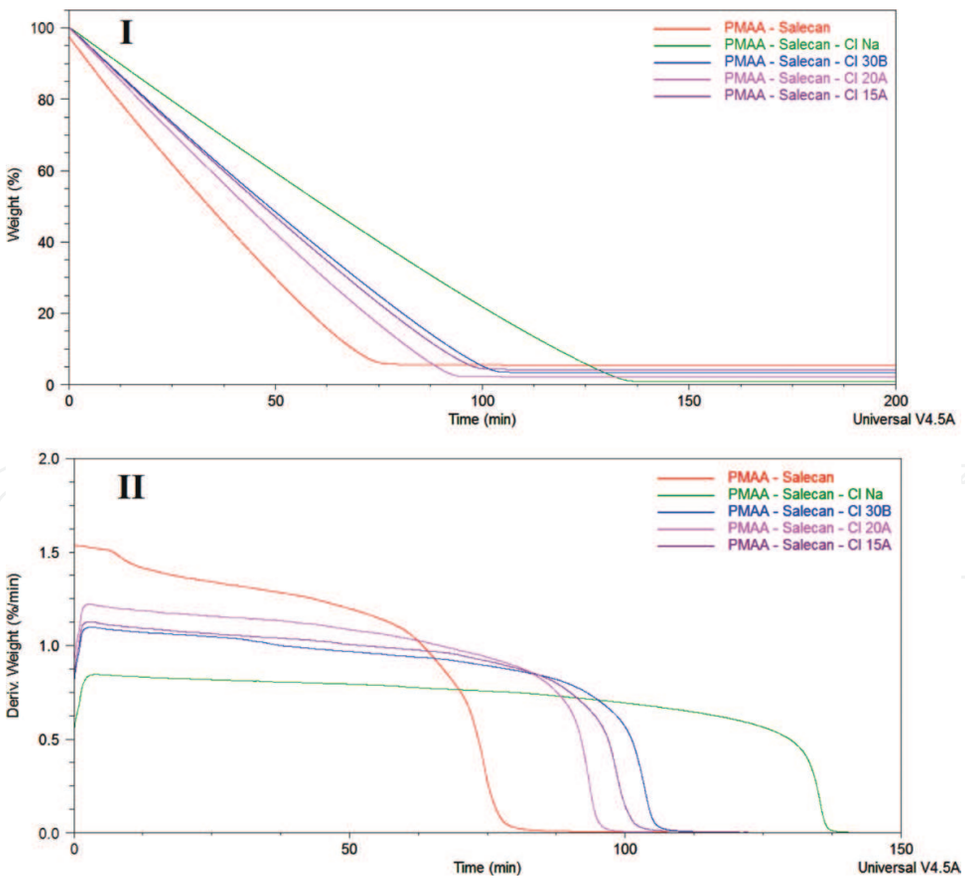

Figure 5. I. Weight loss as a function of time measured at constant temperature (37°C) of the equilibrium swollen hydrogel samples; **II**. Weight derivative as function of time for the equilibrium swollen hydrogel samples; PMAA-Salecan; PMAA-Salecan–ClNa; PMAA-Salecan–Cl30B; PMAA-Salecan–Cl20A; and PMAA-Salecan–Cl15A.

more water compared to the pure hydrogel are as follows: 91.43% water released versus 98.83% (ClNa sample), 96.2% (Cl30B sample), 97.53% (Cl20A sample) and 95.47% (Cl15A) at constant weight. We can notice that the samples with clay lost more water than PMAA-Salecan hydrogel, and PMAA-Salecan-ClNa lost the highest amount of water. This result is well correlated with swelling studies where the PMAA-Salecan-ClNa sample absorbed the largest amount of water. It was previously proved that clay affects the swelling by cross-linking the polymer chains which restricts the mobility of the hydrogel chains [21]. This is a possible explanation for nanocomposite hydrogels which release water later than pure hydrogel. It is worth noting that the time for swelling of the hydrogels is much longer than for deswelling at the same temperature. The collapse time is shifted toward higher values for samples with clay, especially for PMAA-Salecan-ClNa (138.82 min) versus PMAA-Salecan (79.22 min). The conclusion is that the presence of clay layers acts as a barrier in hydrogel networks restricting the release of water over time. This behavior is beneficial for hydrogels where controlled drug release is crucial.

4.5. Scanning electron microscopy and transmission electron microscopy

For the SEM analysis, the synthesized hydrogel cuts were freeze dried. The necessity of performing SEM on lyophilized hydrogels comes from the idea of having the microstructure and morphology of the samples well-retained.

When the samples (see **Figure 6**) were prepared without Salecan, the microstructure of the PMAA/clay hydrogels consists of nonhomogenous areas. A more detailed analysis shows some differences between the nanocomposites, as a function of clay type. When the unmodified montmorillonite (ClNa) is used, the network is clear and more uniform. This confirms the compatibility of the hydrophilic character of clay with the similar nature of the polymer. As for the modified montmorillonite, the more hydrophobic it became, the worse the compatibility with the polymer. Therefore, it can be noticed in case of Cl30B, Cl20A and Cl15A agglomerates of clay layers [22, 23] within the polymeric structure.

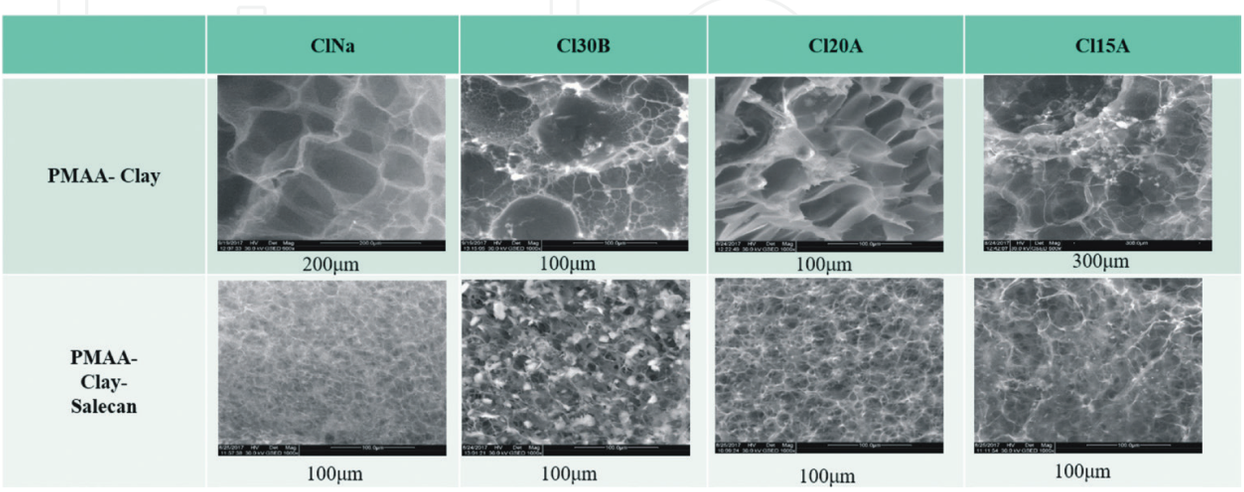

Figure 6. SEM morphology of the PMAA-clay and PMAA-Salecan-clay nanocomposites, respectively. Comparative images obtained for samples with different types of clay.

http://dx.doi.org/10.5772/intechopen.74478

When analyzing the SIPN prepared with Cloisite and Salecan, the microstructure of the examined surfaces consists of dimensionally equivalent voids separated by thin walls. All hydrogels demonstrated homogeneous and porous architectures with the pore size significantly smaller and the pore number became greater [24]. These observations are supported by swelling studies. Thus, when the pore size and number increased, the specific surface became greater resulting in a higher swelling capacity. Differences can be seen between the samples, as another type of Cloisite is used. The morphology of the sample with unmodified clay (ClNa) is a clear and uniform network (similar to the one analyzed before the sample without Salecan). The morphology changes as the hydrophobic (modified) Cloisites participate in the process of developing the nanocomposites. The main change consists of unorganized, crystalline-luminous aggregates of clay, visible on the surface of the samples. From the analysis of the surface, ClNa seems to have a more intercalated or even exfoliated construction, the presumption being confirmed also by XRD analysis.

TEM analyses (see **Figure 7**) prove the existence of intercalated/exfoliated silica lamella within the hydrogel matrix, which was previously presumed by analyzing the XRD results. The internal intercalated structure of the nanocomposites, with the presence of areas with exfoliated clay nanosheets sustains as well the conclusions from the swelling-deswelling studies that showed superior properties for the PMAA-Salecan-ClNa sample.

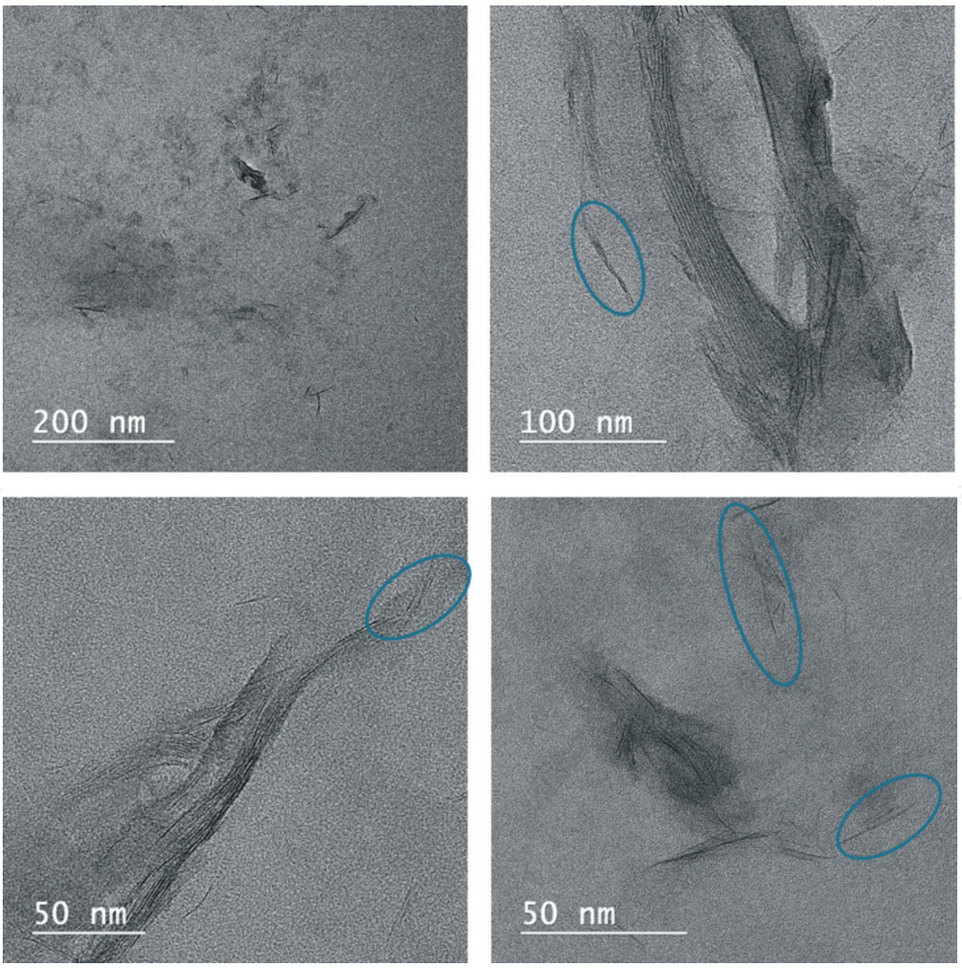

Figure 7. TEM micrographs for PMAA-Salecan-ClNa samples. Exfoliated lamella highlighted with blue circle.

4.6. Thermomechanical properties

In order to appreciate the influence of clay addition, moreover, the effect of clay type upon the mechanical properties of the nanocomposites, dynamic mechanical analyses were performed and are presented in **Figures 8** and **9**. As known from the literature, the storage modulus (G') is considered a way of appreciation of the extent of gel network formation. Thus, a higher G' value means a stronger gel structure.

In absence of Salecan, a simple conclusion can be conceived from the data registered (**Figure 8**). In matter of storage modulus, the inclusion of the inorganic filler leads to stronger microstructure of the hydrogels as function of frequency and time, respectively. The presence of montmorillonite increases the intermolecular forces, and the hydrogel nanocomposite behaves as an elastic solid with an enhanced capacity of storing energy and not breaking under the stress applied. For example, the hydrogels obtained in the presence of Cl20A and Cl15A exhibit higher storage modulus than the neat hydrogel. It is worth mentioning that due to unexpected swelling and disintegration phenomenon that occurred in the washing stage, the samples obtained with ClNa and Cl30B could not be analyzed. Moreover, the stiffness increased with the addition of Cl20A and Cl15A clays proving once again the enhanced mechanical stability of nanocomposite hydrogels induced by the hydrophobic modified silicate nanosheets [25]. The same behavior was observed in our recent study that refers to the obtaining of newly advanced nanocomposite hydrogels based on poly(methacrylic acid) with

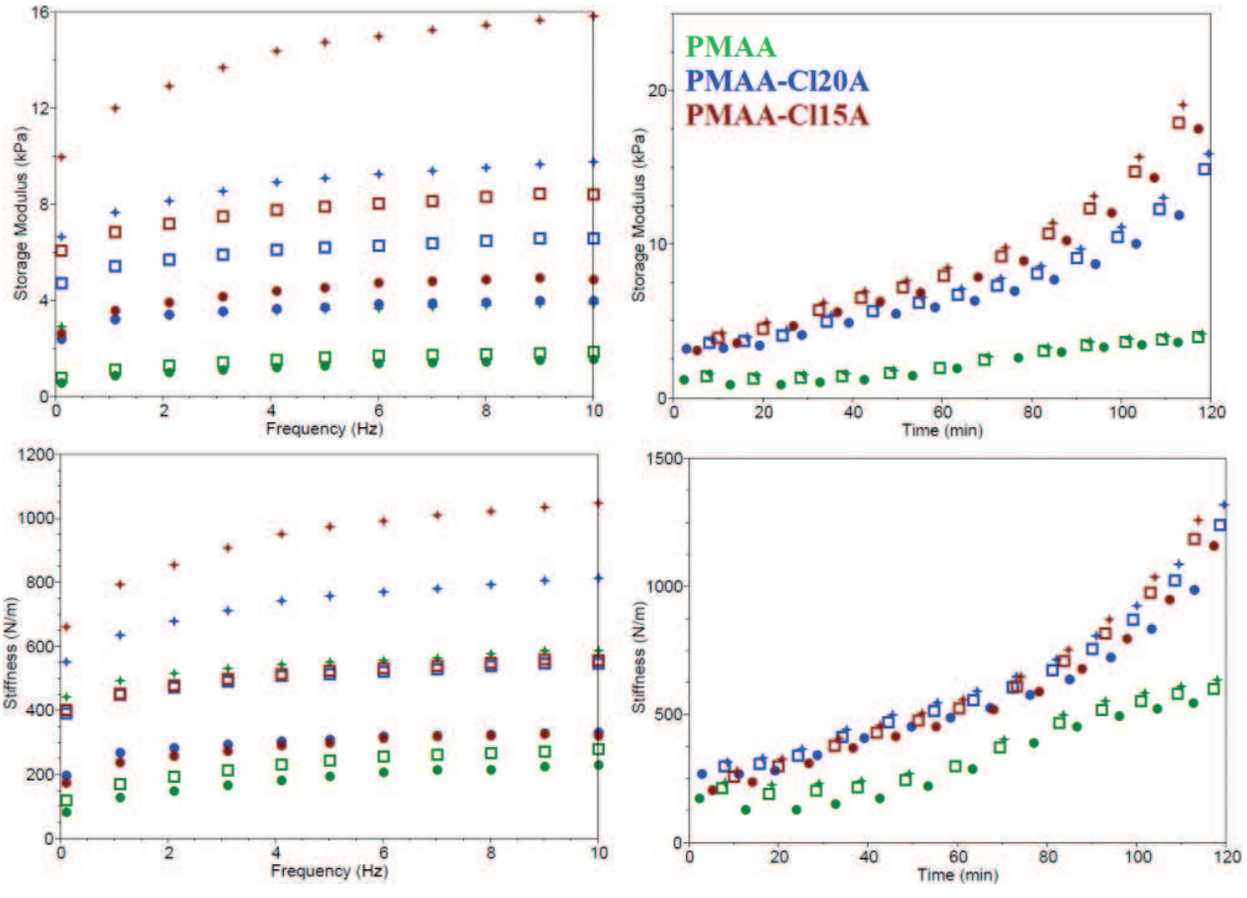

Figure 8. DMA results: storage modulus as a function of frequency and time; stiffness as a function of frequency and time; for: PMAA; PMAA-Cl20A; PMAA-Cl15A.

in house advanced, modified clays by edge covalent bonding [13]. Differences in storage modulus values along frequency-time cycles can be observed due to the hydrogels dehydration.

More challenging to analyze were the results obtained from the samples with Salecan (**Figure 9**). Generally, higher values of storage modulus are noted with the increase in hydrophobicity of the clay used. Thus, even if the storage modulus was lower than for the samples obtained with modified clay, the SIPN containing Cloisite Na were proved to be more stable with frequency and time, in comparison with those obtained with hydrophobic montmorillonites, as observed from the

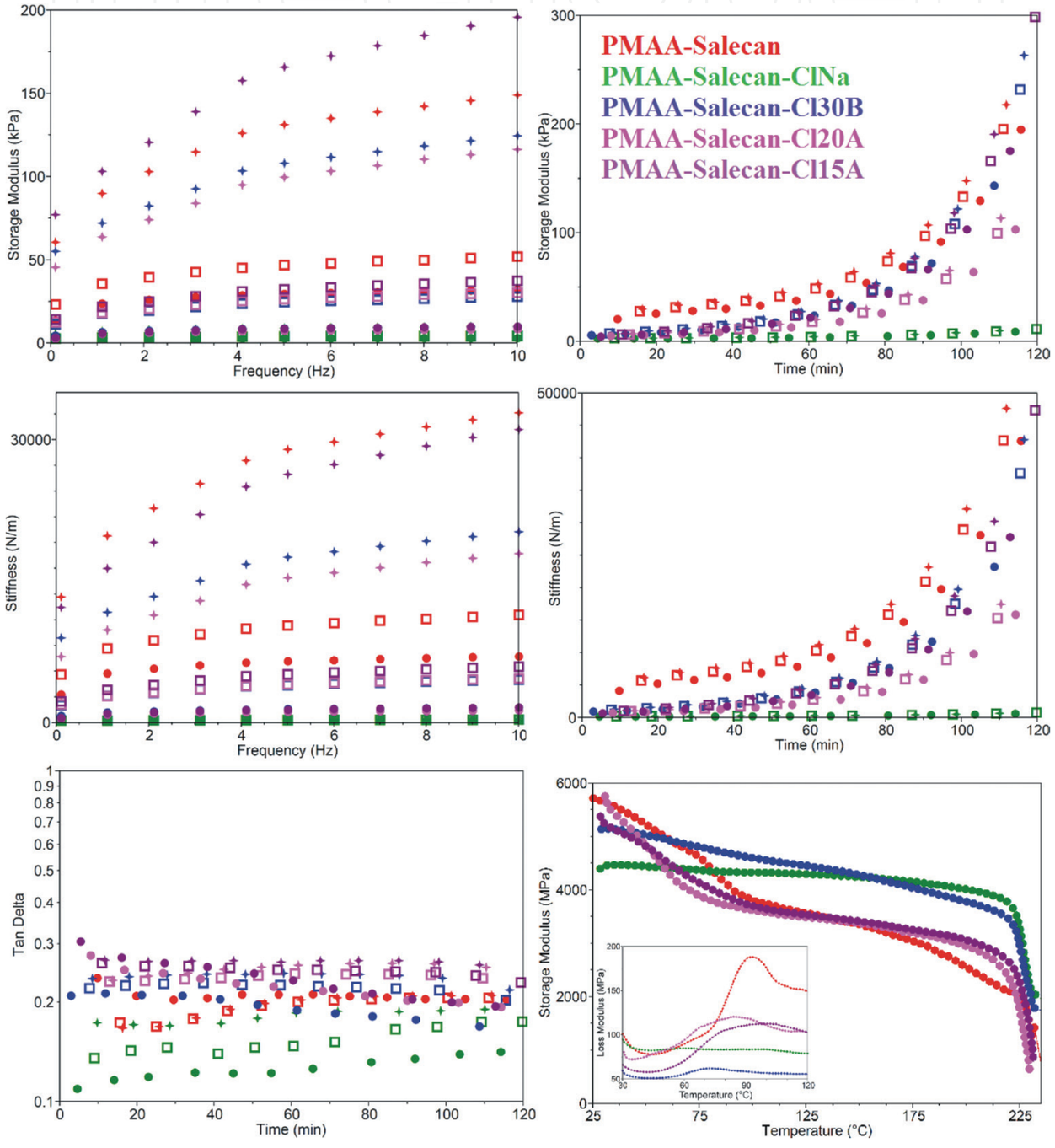

Figure 9. DMA results: storage modulus as a function of frequency and time; stiffness as a function of frequency and time; Tan Delta as a function of time; storage modulus as a function of temperature for: PMAA-Salecan; PMAA-Salecan-ClNa; PMAA-Salecan-Cl30B; PMAA-Salecan-Cl20A; and PMAA-Salecan-Cl15A.

flatness of the specific ClNa curve. These data were in good agreement with swelling-deswelling results where the SIPN with ClNa proved the highest swelling degree and the slowest water release capacity. As a consequence, given the fact that the samples "lose" water when mechanically stressed, the smallest storage modulus values are registered for hydrophilic Cloisites. This phenomenon can also be explained by the presence of a smaller number of silicate sheet in the same volume of the semi-interpenetrated network (the same size of the samples subjected to DMA analysis) as a consequence of the swelling process during washing, which is although an insufficient contribution of silicate lamellae in order to assure an enhanced mechanical behavior.

The DMA analyses obtained for SIPN with Salecan showed increased values for storage modulus and stiffness in comparison with hydrogel nanocomposites. This fact is due to the elastic properties of the Salecan [3, 26, 27] and its –OH groups' interactions with oxygen atoms of the PMAA and the amine protons of the clay as well as between the clay surface hydroxyls and the carbonyl of the polymer. These data are well correlated with FTIR results, peak shifts, respectively, that proved the obtaining of a unique complex structure. Previous studies demonstrated that clay nanoparticles behave as a support for polymer chains which absorb/desorb onto clay sheet by thus inducing a continuous movement in the system [28]. In our case, when applying frequency or time, the whole system reacts trying to withstand, consequently, increased mechanical stability is registered even if the storage modulus was lower than for the samples obtained with modified clay.

For all the hydrogels, tanδ subunitary values indicated that the storage modulus exceeded the loss modulus independent of time, which confirms the elastic solid behavior of the nanocomposites and the dissipation of energy within the whole structure [20].

When temperature increased, the freeze-dried samples evidenced storage modulus changes around 75 and 230°C. These changes are attributed to the movement of methacrylic acid units and are related with the polymer molecular weight. The loss modulus (inset **Figure 9**) registered for SIPN-functionalized clay samples, indicated transition around 70°C due to the melting of quaternary ammonium salts, more obvious in Cl20A and Cl15A cases. The glass transition temperature (around 230°C) does not significantly change when clays were added in the system unlike other cases where the mobility of hydrogel networks was affected, indicating a reinforcing effect of the modified clay [13].

5. Conclusion

Inspired by the recent studies regarding Polymer/Salecan networks and taking into consideration the numerous researches that highlight the outstanding mechanical properties of the clays, we decided to bring an improvement and study the possibility to synthesize PMAA-Salecan hydrogel nanocomposites based on pristine and modified montmorillonite. Further, the effect of the clay type on the final properties of PMAA/Salecan/clay nanocomposites was followed. With the other parameters kept constant, the morphological and compositional analysis performed gave us the possibility of explaining the physicochemical and thermal features of the fabricated materials as function of Cloisite composition.

The designed structures were investigated with the FT-IR technique, which revealed the presence of the specific partner peaks. X-Ray data, supported by TEM images pointed out a

more intercalated structure for the ClNa, which was confirmed by the swelling-deswelling analyses. The presence of exfoliated sheets within the SIPN network prepared with pristine clay was noticed from TEM images. TGA definitely showed that the introduction of Salecan enhanced the thermal stability of the nanocomposites, but no significant distinction was noticed between the samples of different types of inorganic filler. Speaking of mechanical properties, Salecan had a significant impact on the energy dissipation within the semi-IPNs due to its outstanding viscosity properties. The effect of Cloisite and Salecan was expressed by the improved storage modulus and stiffness of the samples.

The more compatible nature of ClNa with the hydrophilic character of PMAA/Salecan hydrogel provided higher swelling capacity, thus slower release in time, which is highly favorable for the designing of a drug release mechanism. As a fact, the smooth architecture of the networks developed with sodium montmorillonite is another reason to believe that the unmodified ClNa would serve as most suitable inorganic filler for the development of an efficient drug release system.

But neither SIPNs obtained with more hydrophobic clays are not to fall and may be employed in controlled *co*-delivery of polar-unpolar drugs. The nontoxicity of the components used sustains the development of semi-IPN architectures with improved mechanical features and adjustable release properties for specific applications in the extensive biomedical domain.

Acknowledgements

This work was supported by a grant of the Romanian National Authority for Scientific Research and Innovation, CNCS/CCCDI-UEFISCDI, project number PN-III-P2-2.1-PED-2016-1896, within PNCDI III.

Conflicts of interest

The authors declare no conflict of interest.

Author details

Tatiana Munteanu[1], Claudia Mihaela Ninciuleanu[2], Ioana Catalina Gifu[2], Bogdan Trica[2], Elvira Alexandrescu[2], Augusta Raluca Gabor[2], Silviu Preda[3], Cristian Petcu[2], Cristina Lavinia Nistor[2], Sabina Georgiana Nitu[2] and Raluca Ianchis[2]*

*Address all correspondence to: ralumoc@yahoo.com

1 Faculty of Applied Chemistry and Materials Science, Politehnica University of Bucharest, Bucharest, Romania

2 National R-D Institute for Chemistry and Petrochemistry ICECHIM, Bucharest, Romania

3 Institute of Physical Chemistry "Ilie Murgulescu", Romanian Academy, Bucharest, Romania

References

[1] Mishra S, Kumar Mishra A. Polymeric hydrogels: A review of recent developments. In: Kalia, Susheel, editors. Polymeric Hydrogels as Smart Biomaterials. Springer Series on Polymer and Composite Materials; 2016. p. 1-17. DOI: 10.1007/978-3-319-25322-0_1

[2] Qi X et al. Development of novel hydrogels based on Salecan and poly(N-isopropylacrylamide-co-methacrylic acid) for controlled doxorubicin release. RSC Advances. 2016;**6**:69869-69881. DOI: 10.1039/C6RA10716H

[3] Qi X et al. Fabrication and characterization of a novel anticancer drug delivery system: Salecan/poly(methacrylic acid) semi-interpenetrating polymer network hydrogel. ACS Biomaterials Science & Engineering. 2015;**1**:1287-1299. DOI: 10.1021/acsbiomaterials.5b00346

[4] Ianchis R et al. Synthesis and properties of new epoxy-organolayered silicate nanocomposites. Applied Clay Science. 2015;**103**(Supplement C):28-33

[5] Nagahama K et al. Self-assembling polymer micelle/clay nanodisk/doxorubicin hybrid injectable gels for safe and efficient focal treatment of cancer. Biomacromolecules. 2015;**16**(3):880-889

[6] Pinnavaia TJ, Beall GW. Polymer-Clay Nanocomposites. Wiley; 2000. 370 p. ISBN: 978-0-471-63700-4

[7] Ianchis R et al. Polymer-clay nanocomposites obtained by solution polymerization of vinyl benzyl triammonium chloride in the presence of advanced functionalized clay. Nanomaterials. 2014;**126**:609-616. DOI: 10.3390/nano7120443

[8] Corobea MC et al. Silica nanowires obtained on clay mineral layers and their influence on mini-emulsion polymerisation. Applied Clay Science. 2014;**95**:232-242

[9] Park JK et al. Controlled release of donepezil intercalated in smectite clays. International Journal of Pharmaceutics. 2008;**359**(1):198-204

[10] Galimberti M et al. Clay delamination in hydrocarbon rubbers. 2007;**19**:2495-2499

[11] Sinha Ray S, Okamoto M. Polymer/layered silicate nanocomposites: A review from preparation to processing. Progress in Polymer Science. 2003;**28**:1539-1641. DOI: doi.org/10.1016/j.progpolymsci.2003.08.002

[12] Ianchis R et al. Implications of silylated montmorillonite on montmorillonite–polyacrylate nanocomposites. Applied Clay Science. 2011;**52**(1):96-103

[13] Donescu D, Ianchis R, Petcu C, Purcar V, Nistor CL, Radovici C, Somoghi R, Pop SF, Perichaud A. Study of the solvents influence on the layered silicates-cation polymer hybrids properties. Digest Journal of Nanomaterials and Biostructures. 2013;**8**(4):1751-1759

[14] Ianchis R, Corobea MC, Donescu D, Rosca ID, Cinteza LO, Nistor LC, Vasile E, Marin A, Preda S. Advanced functionalization of organoclay nanoparticles by silylation and their polystyrene nanocomposites obtained by miniemulsion polymerization. Journal of Nanoparticle Research. 2012;**14**:1233-1244. DOI: 10.1007/s11051-012-1233-6

[15] Ianchis R, Donescu D, Petcu C. Influence of layered silicate on microemulsion polymerization kinetics of butylacrylate with alkoxylane. Materiale Plastice. 2008;**45**(3):265-268

[16] Bajpai SK, Chand N, Mahendra M. In situ formation of silver nanoparticles in poly (methacrylic acid) hydrogel for antibacterial applications. Polymer Engineering & Science. 2013;**53**(8):1751-1759

[17] Qi X et al. Investigation of Salecan/poly(vinyl alcohol) hydrogels prepared by freeze/thaw method. Carbohydrate Polymers. 2015;**118**(Supplement C):60-69

[18] Pretsch E, Bühlmann P, Badertscher M. Structure Determination of Organic Compounds: Tables of Spectral Data. th4 ed. Berlin Heidelberg: Springer-Verlag; 2009. pp. 433-447

[19] Russo P et al. Structure and physical properties of high amorphous polyvinyl alcohol/clay composites. AIP Conference Proceedings. 2015;**1695**:020035. DOI: doi.org/10.1063/1.4937313

[20] Wei W et al. A novel thermo-responsive hydrogel based on salecan and poly(N-isopropylacrylamide): Synthesis and characterization. Colloids and Surfaces. B, Biointerfaces. 2015;**125**:1-11

[21] Zheng S et al. Fast deswelling and highly extensible poly(N-isopropylacrylamide)-hectorite clay nanocomposite cryogels prepared by freezing polymerization. Polymer. 2013;**54**(7):1846-1852

[22] Ianchis R et al. Surfactant-free emulsion polymerization of styrene in the presence of silylated montmorillonite. Applied Clay Science. 2009;**45**(3):164-170

[23] Manfredi L et al. Influence of clay modification on the properties of resol nanocomposites. Macromolecular Materials and Engineering. 2008;**293**:878-886. DOI: 10.1002/mame.200800158

[24] Fathy F. Preparation of carboxymethyl cellulose-g-poly(acrylic acid-2-acrylamido-2-methylpropane sulfonic acid)/attapulgite superabsorbent composite. American Journal of Polymer Science and Technology. 2016;**2**:11-19. DOI: 10.11648/j.ajpst.20160201.12

[25] Han L et al. Mussel-inspired adhesive and tough hydrogel based on nanoclay confined dopamine polymerization. ACS Nano. 2017;**11**(3):2561-2574

[26] Hu X et al. Synthesis and characterization of a novel semi-IPN hydrogel based on Salecan and poly(N,N-dimethylacrylamide-co-2-hydroxyethyl methacrylate). Carbohydrate Polymers. 2014;**105**(Supplement C):135-144

[27] Xiu A et al. Rheological properties of Salecan as a new source of thickening agent. Food Hydrocolloids. 2011;**25**:1719-1725. DOI: doi.org/10.1016/j.foodhyd.2011.03.013

[28] Zhao LZ et al. Recent advances in clay mineral-containing nanocomposite hydrogels. Soft Matter. 2015;**11**(48):9229-9246

IntechOpen